Contract FP6-IST 508009

ACE

Antenna Centre of Excellence

Instrument: Network of Excellence

Thematic Priority: IST - Information Society Technologies
Mobile and wireless systems beyond 3G

Deliverable A1.2D4
Recommended practices for Near Field measurements

Due date of deliverable: 30/06/2005
Actual submission date: 30/06/2005

Start date of project: 1/1/2004 Duration: 24 months

Organisation name of lead contractor for this deliverable: SATIMO

Revision 1.0

Document Number: FP6-IST-508009-A1.2D4

Work package: 1.2-4

Estimated Person Months: 7

Dissemination level (PU,PP,RE,CO): PU (Public)

Nature (R, P, D, O): R (Report)

Version: 1

Total Number of Pages: 33

File name: WP1.2D4.pdf

Editors: Lars Foged (Satimo), Sergey Pivnenko (TUD), Aksel Frandsen (Ticra)

Participants: Lars Foged (Satimo), Sergey Pivnenko (TUD), Aksel Frandsen (Ticra)

Abstract

In 2003 the Antenna Standards Committee under the auspices of IEEE (The Institute of Electrical and Electronics Engineers, Inc.) initiated an effort to develop recommended practices for general near-field antenna measurements. This effort has been joined by US organizations and companies, and the activity coordinated by ACE ensures that European institutions and companies are involved in this work and are actively contributing to the standard. The IEEE committee meets in the US twice a year to plan and coordinate the activities. The standardisation work under IEEE is presently moving into the initial writing phase and has four years available to arrive at a consolidated standard. At present, an outline for a document on recommended practices has been drafted, and responsible parties have been assigned to each paragraph.

The ACE partners (Satimo, TUD and Ticra) involved in this activity are contributing actively to all areas of the standardisation and each member has been assigned the responsibility of paragraphs of the standard. The contributions are in the area of spherical near field antenna measurements, near field probes and probe arrays. This document summarises and further expands the contributions from the ACE partners in the above fields.

This self standing document recommends on near-field measurement practices for spherical geometries. It also recommends on measurement practices for the calibration of probes and probe arrays in near-field measurements.

Keyword List

Near Field, Antenna Measurements, Standards, Recommendations

Document Evolution

Revision	Date	Reason of change
Rev. 1.0	30/06/2005	First Edition

Table of contents

1 Introduction

1.1 Scope

In 2003 the Antenna Standards Committee under the auspices of IEEE (The Institute of Electrical and Electronics Engineers, Inc.) initiated an effort to develop recommended practices for general near-field antenna measurements. This effort has been joined by US organizations and companies, and the activity coordinated by ACE ensures that European institutions and companies are involved in this work and are actively contributing to the standard. The IEEE committee meets in the US twice a year to plan and coordinate the activities. The standardisation work under IEEE is presently moving into the initial writing phase and has four years available to arrive at a consolidated standard. At present, an outline for a document on recommended practices has been drafted [3], and responsible parties have been assigned to each paragraph.

The ACE partners (Satimo, TUD and Ticra) involved in this activity are contributing actively to all areas of the standardisation and each member has been assigned the responsibility of paragraphs of the standard. The contributions are in the area of spherical near field antenna measurements, near field probes and probe arrays. This document summarises and further expands the contributions from the ACE partners in the above fields.

This self standing document recommends on near-field measurement practices for spherical geometries. It provides information on developments in spherical near-field antenna measurements that have occurred since the writing of IEEE Std 149-1979 (IEEE Standard Test Procedures for Antennas) [1]. It also recommends on measurement practices for the calibration of probes and probe arrays in near-field measurements.

1.2 Antenna Patterns

We consider an $e^{-i\omega t}$ time dependence with frequency $f = \omega/(2\pi)$, wave number $k = 2\pi/\lambda$, and wavelength λ. Sufficiently distant from a radiating antenna, the electric field is given by the expression:

$$\boldsymbol{E}_t(\boldsymbol{r}) \underset{r\to\infty}{\sim} \boldsymbol{t}(\hat{\boldsymbol{r}})\,\frac{e^{ikr}}{ikr}\,a_0 \tag{1.1}$$

$$\boldsymbol{r}\cdot\boldsymbol{t}(\hat{\boldsymbol{r}}) = 0 \tag{1.2}$$

In any direction, the *transmitting function* $\boldsymbol{t}(\hat{\boldsymbol{r}})$ is characterized by amplitude and phase (or real and imaginary parts) and polarization. Equation (1.1) embodies the linear relation between the radiated field and the excitation a_0. The power accepted by the antenna is:

$$P_0 = K_t(1-|\,\Gamma_t\,|^2)\,|\,a_0\,|^2 \tag{1.3}$$

where Γ_t is the reflection coefficient looking into the transmitting antenna, and K_t is an arbitrary constant. Once K_t is fixed, P_0 determines a_0, and hence $\boldsymbol{t}(\hat{\boldsymbol{r}})$, up to an arbitrary (and unimportant) overall phase factor.

A common rule of thumb states that (1.1) is valid in the *far-field region* $r > r_f$ where

$$r_f \sim \frac{2D^2}{\lambda} \tag{1.4}$$

and D is the diameter of the smallest sphere that encloses the active parts of the antenna. Larger values of r_f may be needed to satisfy accuracy requirements.
Consider an incident plane wave

$$\boldsymbol{E}_i(\boldsymbol{r}) = \frac{\boldsymbol{E}_0}{2\pi} e^{i\boldsymbol{k}\cdot\boldsymbol{r}} \tag{1.5}$$

$$\boldsymbol{k}\cdot\boldsymbol{E}_0 = 0, \quad \boldsymbol{k}\cdot\boldsymbol{k} = k^2 \tag{1.6}$$

The response of a receiving antenna is given in terms of the *receiving function* $\boldsymbol{s}(\hat{\boldsymbol{k}})$:

$$b_0 = \boldsymbol{s}(\hat{\boldsymbol{k}})\cdot\boldsymbol{E}_0 \tag{1.7}$$

The received power is

$$P_r = K_r \,|\, b_0 \,|^2 \tag{1.8}$$

Here K_r is an arbitrary constant, and the load is assumed to be non-reflecting. To be definitive, we use the normalizations

$$K_t = K_r = \frac{1}{2k^2 Z_0} \tag{1.9}$$

where $Z_0 = \sqrt{\mu_0 / \varepsilon_0} \approx 377\Omega$ is the impedance of free space. With this choice, a_0 and b_0 have the dimensions of electric field [V/m], and the transmitting and receiving functions are dimensionless. Following IEEE Std 145-1993 [2], directional *gain* and *effective area* are given by

$$G(\hat{\boldsymbol{r}}) = \frac{4\pi}{1 - |\,\Gamma_t\,|^2} \,|\, \boldsymbol{t}(\hat{\boldsymbol{r}}) \,|^2 \tag{1.10}$$

$$\sigma(\hat{\boldsymbol{r}}) = \frac{\lambda^2}{1 - |\,\Gamma_r\,|^2} \,|\, \boldsymbol{s}(\hat{\boldsymbol{r}}) \,|^2 \tag{1.11}$$

Here Γ_r is the reflection coefficient looking into the receiving antenna. Also when (1.9) is adopted, reciprocity implies that

$$\boldsymbol{s}(\hat{\boldsymbol{r}}) = \boldsymbol{t}(-\hat{\boldsymbol{r}}) \tag{1.12}$$

or

$$\sigma(\hat{\boldsymbol{r}}) = \frac{\lambda^2}{4\pi} G(-\hat{\boldsymbol{r}}) \tag{1.13}$$

Throughout this document, we assume that the antenna under test is a passive, linear, reciprocal device. Consequently, it can be measured in either the transmitting or receiving mode. However, many of the test practices can be adapted for measuring antennas with active, non-linear, or non-reciprocal components.

We also use the term *pattern* to refer to the transmitting or receiving function when a specific normalization is not implied. A pattern can be normalized easily to satisfy (1.10) or (1.11) if the gain or directivity is known in some direction.

2 Summary of spherical near field measurement theory

The theoretical basis for all antenna testing techniques is a transmission formula, which expresses the signal received by an antenna when another antenna is transmitting. The receiving characteristics of the first antenna as well as the transmitting characteristics of the second antenna enter into the transmission equation. Assuming reciprocity, it does not matter which of the two antennas transmits and which receives. In practice, however, restrictions may be imposed on the antenna to be tested, e.g. it may only operate in receive mode.

In spherical near-field antenna testing one utilizes the fact that each of the two antennas involved in the measurement, the Antenna Under Test (AUT) and the auxiliary antenna, the Probe, can be characterized by a finite, discrete set of coefficients, which expresses the radiation, and - due to reciprocity - the receiving properties of the antenna. These coefficients are the weight factors in a truncated expansion of the antenna radiation in spherical vector waves. This expansion satisfies Maxwell's equations.

2.1 Basic theory

Whereas a complete and thorough exposition of spherical near-field antenna testing may be found in Hansen's authoritative book [5] on the subject we will in this Chapter confine ourselves to the most essential and omit many details.

2.2 Spherical wave expansion

A Spherical Wave Expansion (SWE) of the electric field radiated by an antenna into free space may be defined as a weighted sum of spherical vector wave functions

$$\vec{E}(r,\theta,\phi)=\frac{k}{\sqrt{\eta}}\sum_{smn} Q_{smn}\vec{F}_{smn}(r,\theta,\phi) \tag{2.1}$$

where the Q_{smn}'s are the complex expansion coefficients, k the wavenumber, $k=2\pi/\lambda$, λ being the wavelength, η is the free-space specific admittance, and (r,θ,ϕ) are the usual spherical coordinates. In Eq. (2.1) the triple summation shall be understood as

$$\begin{aligned}\sum_{smn} &\triangleq \sum_{s=1}^{2}\sum_{n=1}^{N}\sum_{m=-n}^{m=+n} \\ &= \sum_{s=1}^{2}\sum_{m=-N}^{m=N}\sum_{n=\max(1,|m|)}^{N}\end{aligned} \tag{2.2}$$

The spherical vector wave functions $\vec{F}_{smn}(r,\theta,\phi)$ are defined as follows :

$$\begin{aligned}\vec{F}_{1mn}(r,\theta,\phi) = &\left(-\frac{m}{|m|}\right)^m \frac{1}{\sqrt{2\pi}} \frac{1}{\sqrt{n(n+1)}} \\ &\left\{ h_n^{(1)}(kr) \frac{im\bar{P}_n^{|m|}(\cos\theta)}{\sin\theta} e^{im\phi}\hat{\theta} \right. \\ &\left. -h_n^{(1)}(kr) \frac{\mathrm{d}\bar{P}_n^{|m|}(\cos\theta)}{\mathrm{d}\theta} e^{im\phi}\hat{\phi} \right\}\end{aligned} \tag{2.3}$$

and

$$\begin{aligned}\vec{F}_{2mn}(r,\theta,\phi) = &\left(-\frac{m}{|m|}\right)^m \frac{1}{\sqrt{2\pi}} \frac{1}{\sqrt{n(n+1)}} \\ &\left\{ \frac{n(n+1)}{kr} h_n^{(1)}(kr) \bar{P}_n^{|m|}(\cos\theta) e^{im\phi}\hat{r} \right. \\ &+ \frac{1}{kr} \frac{\mathrm{d}}{\mathrm{d}(kr)} \left(krh_n^{(1)}(kr) \right) \frac{\mathrm{d}\bar{P}_n^{|m|}(\cos\theta)}{\mathrm{d}\theta} e^{im\phi}\hat{\theta} \\ &\left. + \frac{1}{kr} \frac{\mathrm{d}}{\mathrm{d}(kr)} \left(krh_n^{(1)}(kr) \right) \frac{im\bar{P}_n^{|m|}(\cos\theta)}{\sin\theta} e^{im\phi}\hat{\phi} \right\}\end{aligned} \tag{2.4}$$

where we have assumed - and suppressed - a time dependence of $e^{-i\omega t}$. In Eqs. (2.3) and (2.4), $h_n^{(1)}(kr)$ is the spherical Hankel function of the first kind, corresponding to outward wave propagation, while $\bar{P}_n^{|m|}(\cos\theta)$ is the normalized associated Legendre function. There are other possible notations in use, but the present choice of wave functions has some advantages, among which one finds a particularly simple expression for the radiated power from the antenna. In this notation any single radiated spherical wave with unit amplitude will radiate a power of ½ watt. Therefore the expansion above is denoted a power-normalized Spherical Wave Expansion, where the wave functions $\vec{F}_{smn}(r,\theta,\phi)$ are dimensionless, and the dimension of the expansion coefficients Q_{smn} becomes [watt]^{½}. The total power radiated from the test antenna then becomes

$$P_{rad} = \frac{1}{2} \sum_{smn} |Q_{smn}|^2 \tag{2.5}$$

2.2.1 Minimum sphere and mode truncation

The expansion in Eq. (2.1) is valid in a source-free region outside the *minimum sphere*, which is defined as the smallest spherical surface with its centre in the origin of the coordinate system and completely enclosing the antenna. Traditionally the radius of this sphere is denoted r_o. Note that the AUT does not necessarily need to be centred in the spherical coordinate system, although this position will result in the smallest minimum sphere.

The determination of the upper truncation limit, $N = \max(n)$, in the SWE in Eqs. (2.1) and (2.2) is closely related to the size of the minimum sphere and the cut-off properties of the spherical Hankel functions $h_n^{(1)}(kr)$. Leaving out the details, the maximum summation index in n, N, is customarily given by the empirical rule

$$N = [kr_o] + n_1 \tag{2.6}$$

where [ ] represents the integer closest to kr_o and n_1 is an integer which depends on the positions of the sources within the minimum sphere, the distance from the minimum sphere at which the field is evaluated, as well as on the requirements to accuracy. If the evaluation distance is more than a few wavelengths from the minimum sphere, early numerical studies have shown that a value of $n_1 = 10$ will be adequate for most practical purposes.

However, with still increasing antenna sizes, tighter requirements to accuracy, and the vast speed and capacity increase of computers, a need for a revision of the truncation limit has emerged. Recently, a more elaborate estimate for the truncation limit, N, has been devised [8]. This revised truncation criterion reads

$$N = [kr_o] + n_2 \tag{2.7}$$

where n_2 is given by

$$n_2 = \max\left(\left[A \cdot \sqrt[3]{kr_o}\right], 10\right) \tag{2.8}$$

and A is an empirically determined factor which depends on the required accuracy. The minimum value of 10 for n_2 caters for small antennas, in accordance with Eq (2.6). For a relative accuracy level of -80 dB, $A = 3.6$, while $A = 5.0$ for a -100 dB relative accuracy.

In the treatment above, only the truncation of the expansion imposed by the size of the minimum sphere was treated, i.e. truncation in the polar index n. However, in certain cases the expansion can also be truncated in the azimuthal index m, at some $|m| = M$, where $M < N$. This will be dealt with later.

2.2.2 Transmission formula

The *transmission formula* is the fundamental basis for spherical near-field antenna testing. As in planar near-field scanning, the interaction between a test antenna and the probe in the near-field may conveniently be analysed using the scattering matrix theory of antennas [9], [10] and [11].

The formula expresses the complex signal received by a probe with known receiving characteristics as a function of the probe coordinates (A, θ, ϕ) and the probe rotation angle χ, when a test antenna with unknown radiation characteristics transmits. Figure 1 shows schematically the AUT and probe minimum spheres and their associated coordinate systems. The derivation of the transmission

formula involves fairly complex mathematical operations with spherical vector waves under rotation and translation of coordinate systems, and will not be detailed here. Interested readers are referred to [5].

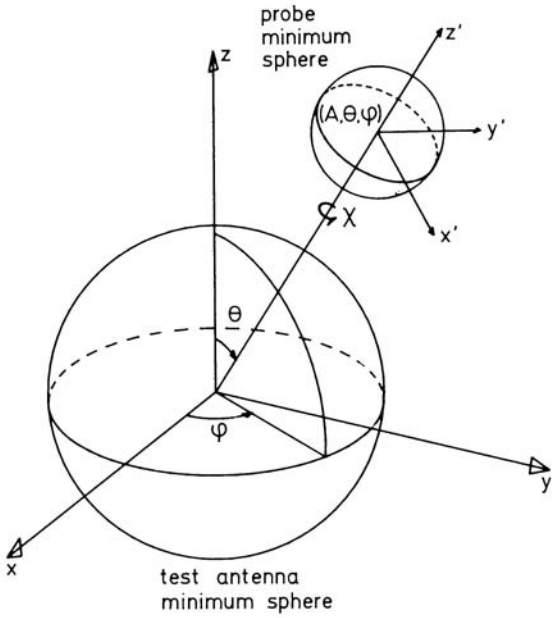

Figure 1: Test antenna and probe minimum spheres (from [5], with permission)

The signal $w(A,\chi,\theta,\phi)$ received by the probe antenna may be written in the form

$$w(A,\chi,\theta,\phi)=v\sum_{smn\mu}T_{smn}e^{im\phi}d^{n}_{\mu m}(\theta)e^{i\mu\chi}P_{s\mu n}(kA) \tag{2.9}$$

where

$$P_{s\mu n}(kA)=\frac{1}{2}\sum_{\sigma\nu}C^{sn}_{\sigma\mu\nu}(kA)R^{p}_{\sigma\mu\nu} \tag{2.10}$$

are the *probe response constants*, which are known once the probe receiving coefficients $R^{p}_{\sigma\mu\nu}$ have been determined. The Greek indices (σ,μ,ν) in the above summations relate to the probe, in the same manner as the Latin indices (s,m,n) relate to the test antenna. The $d^{n}_{\mu m}(\theta)$ and $C^{sn}_{\sigma\mu\nu}(kA)$ are well-defined rotation and translation coefficients, respectively. The T_{smn}'s are the sought-for quantities for the AUT, while v represents the complex excitation of the AUT. The relation between the Q_{smn}'s in Eq. (2.1) and the T_{smn}'s in Eq. (2.9) is [5].

$$Q_{smn}=vT_{smn} \tag{2.11}$$

As is common practice in derivations leading to the transmission formulas, multiple reflections (interactions) between the AUT and probe are assumed to be negligible, and are therefore ignored. Their inclusion in the formulation would require a complete knowledge of the AUT and probe scattering matrices, not only their transmitting and receiving parts.

3 Implementation

The main problem in spherical near-field antenna testing is the determination of the AUT's transmitting (or receiving) coefficients from measurements carried out in its near field, i.e. from the measured probe signal $w(A,\chi,\theta,\phi)$, the transmission formula (Eq. (2.9)) must be 'inverted' to find the T_{smn}'s. In solving for the T_{smn}'s the influence of the probe shall be accounted for through a *probe correction*. With a knowledge of the T_{smn}'s the field radiated from the AUT may be evaluated anywhere outside the minimum sphere, in particular in the far field, which is typically what is required in most applications.

Since the measured signal $w(A,\chi,\theta,\phi)$ on the left-hand side of Eq. (2.9) for practical and obvious reasons is not a continuous function, but merely consists of a discrete set of recorded data, the inversion of the transmission formula in a computer requires discretization as well. Counting the number of terms in the summation Eq. (2.2) one finds that there are $2N\left(N+2\right)$ unknown T_{smn} coefficients, and hence *at least* the same number of discrete measurement samples must be present in order to solve for the AUT transmitting coefficients.

The transmission formula may of course be solved numerically by *brute force,* simply by forming a system of linear equations by inserting at least $2N\left(N+2\right)$ discrete samples of $w(A,\chi,\theta,\phi)$ in Eq. (2.9), but this is cumbersome, time-consuming and not very efficient for practical AUTs, where the maximum index N (Eqs. (2.6)-(2.7)) can easily be considerably larger than 100, thus putting severe demands on computer memory. This approach may possibly also lead to ill-conditioned systems.

An efficient algorithm to solve the transmission formula has been proposed in [10], [12], [14] and improved and implemented in [11]. The algorithm employs advanced data reduction techniques in combination with Fast Fourier Transforms, and is thus very efficient. The detailed derivations and steps in the algorithm may be found in [5].

As formulated, the algorithm does not impose restrictions on the probe in terms of its content of spherical harmonics. In each (A,θ,ϕ) sample point on the measurement sphere, the near-field must be measured for as many χ-positions of the probe as there are significant, azimuthal μ-harmonics in the probe's radiation pattern. However, as pointed out in [10], if the probe is restricted to only possess two harmonics in its azimuthal pattern, namely harmonics with $\mu=\pm 1$, corresponding to a $\cos\phi$ and $\sin\phi$ azimuthal variation, the algorithm becomes extremely efficient even for *very* large AUTs. The $\mu=\pm 1$ restriction on the probe does not present a severe limitation, since such a probe can easily be constructed. A circular waveguide, smooth-walled or corrugated conical horn excited with the fundamental TE_{11} cylindrical waveguide mode fulfils this condition. An additional advantage for such a probe is the ability to make it *dual-polarized*, which reduces the measurement time by a factor of 2, since both the θ- and the ϕ-component of the field can be measured simultaneously, e.g. by using a switch between the two probe ports.

Recently, in [13] an alternative algorithm has been proposed for probe corrected spherical near-field antenna measurements using so-called *odd-order* probes, which are probes containing azimuthal harmonics with $\mu = \pm 1, \pm 3, \pm 5, ..., \pm \mu_{\max}$. This extends the family of probes that may be used in spherical near-field measurements, so that e.g. rectangular waveguides and horns may also find use. As opposed to the *Wacker/Jensen/Larsen* algorithm for such a probe, it is only necessary to measure the θ- and ϕ-components for two χ-positions of the probe, $\chi = 0^\circ$ and $\chi = 90^\circ$. The implementation of this algorithm in an operational spherical near-field measurement facility has not yet been completed, so presently there is no experience with efficiency, accuracy and other practical measurement related aspects.

4 Measurement set-up

As for any antenna test range, a spherical near-field antenna measurement range consists of several subsystems,

- the mechanical system,
- the electrical (RF) system,
- the data-collecting and controlling system (DCCS)
- the data-processing system.

The mechanical system shall provide for the three axes of rotation corresponding to the three angular variables (χ,θ,ϕ) in Eq. (2.9). Figure 2 illustrates the general spherical near-field set-up.

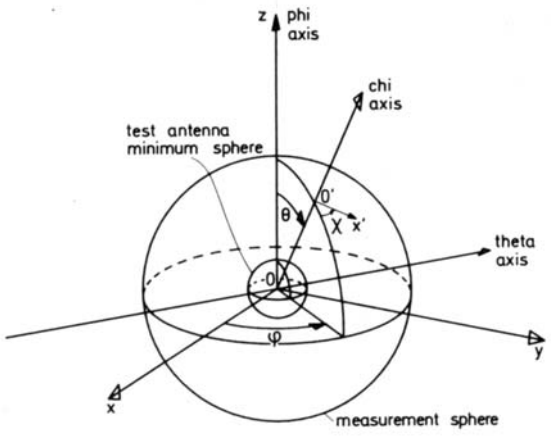

Figure 2 Geometry of general spherical near-field set-up.
(from [5], with permission)

At any point on the spherical measurement surface (A,θ,ϕ) the probe must point to the centre of the sphere and sample two orthogonal polarizations, corresponding to two values of χ. In principle it does not matter which of the two antennas moves relative to the other: The AUT may be fixed, with all rotations being done by the probe, the AUT may rotate around two axes with the probe rotating around the χ-axis, or the AUT may rotate around one axis with the probe rotating around two axes. If the probe is dual-polarized, there is no need for rotating the probe in χ. The actual implementation of the mechanical system can be done in a multitude of ways, with varying degrees of mechanical complexity, ranging from a fairly simple *elevation-over-azimuth* set-up to complex *double-gantry arm* systems. Systems employing probes on telescopic and/or robotic arms have also been implemented. The advantage of the latter systems is their flexibility and the ability to accommodate also the planar and cylindrical scanning geometries. High speed measurement systems employing only one mechanical axis of rotation in ϕ , and a circular arch with a series of dual-polarized scattering dipoles providing electrical 'rotation' in θ and χ are also feasible set-ups for spherical near-field antenna testing.

The mounting of the AUT in the set-up is usually dictated by mechanical considerations, either enforced by the mechanical system *per se* and/or by the AUT's mechanical interface. Restrictions on how the AUT may be moved and rotated may also influence the choice of mounting. Traditionally the orientation of the AUT is either *pole pointing* or *equator pointin*g as illustrated in Figure 3, where the AUT is depicted as a circular aperture antenna. Parts of the measurement grid are also shown.

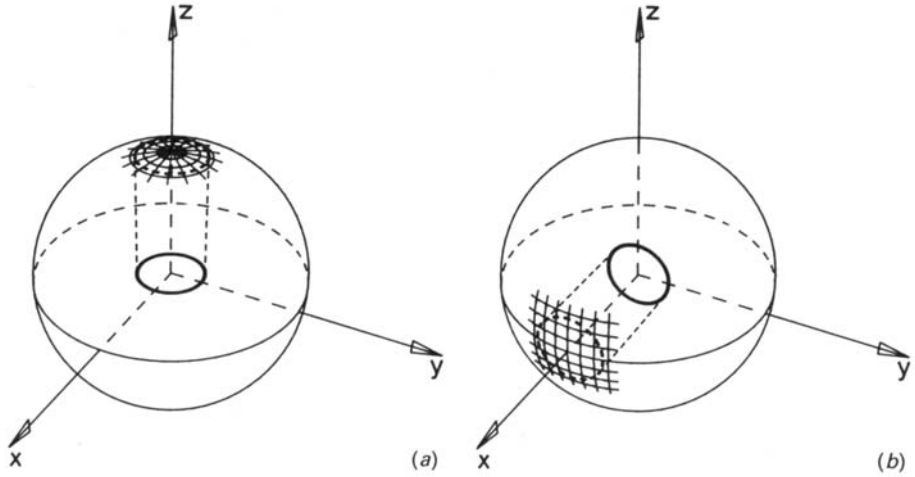

Figure 3: Orientation of AUT in measurement coordinate system.
(a) polar pointing, (b) equator pointing (from [5], with permission)

The RF subsystem comprises the signal source, a receiver which can measure both amplitude and phase, the probe, and cables and circuitry to connect the various parts. Both short- and long-term stability of the RF system during scanning of the AUT is very critical for the accuracy of the measurements.

The data-collection and control system monitors and controls all the instruments and positioning systems in the set-up. Since this is a very complex system, an automated and fully computer-controlled DCCS is required. Similarly the data-processing system must be able to handle and keep track of very large amounts of measured and processed data, which calls for high capacity computers.

4.1 Sampling criteria

The number of significant spherical modes present in the field radiated from the AUT depends on the size of the antenna, as stated in Section 2.2.1. The algorithm for inversion of the transmission formula (Eq. (2.9)) defines the sampling scheme to be used during the scanning of the AUT near field. The sampling is equidistant in θ and ϕ which is a prerequisite for using the Fast Fourier Transform (FFT) techniques. The FFT in turn ensures a very efficient algorithm.

On the other hand the equidistant sampling leads to an oversampling of the field, compared to what is actually required, but from a practical point of view, equidistant sampling is to be preferred to non-equidistant sampling, where the sampling would be 'thinned' close to the poles at $\theta = 0^\circ$ and $\theta = 180^\circ$.

When the expansion of the field radiated from the AUT can be truncated at N, then the fastest variation in θ is $e^{\pm iN\theta}$, and hence a sampling interval of

$$\Delta\theta = \frac{180^\circ}{N} \tag{4.1}$$

or less will be sufficient. Furthermore, since $\max(|m|) \leq N$, the maximum sampling interval in ϕ is the same, i.e.

$$\Delta\phi = \Delta\theta \tag{4.2}$$

However, in many cases a larger value of $\Delta\phi$ may be used, if e.g. the AUT possesses some degree of symmetry. Assuming e.g. that the antenna can be enclosed by a minimum cylinder with its axis coincident with the z-axis and with a radius $R_o \left(\leq r_o\right)$. Then the upper limit on $|m|$ is close to $kR_o + 10$. Further reduction in the upper limit on $|m|$ is possible if one is only interested in the field within a certain angular region around the pole at $\theta = 0^\circ$. The latter is a consequence of the cut-off properties of the associated Legendre functions. Examples are rotational symmetric antennas with their axis of rotation coinciding with the z-axis, and where the antenna excitation contains azimuthal harmonics $e^{\pm im\phi}, m = 0,1,2,....,M$, only. For a directive antenna pointing towards the equator plane of the measurement grid (i.e. at $\theta = 90^\circ$), one must choose $\Delta\phi = \Delta\theta$.

When projected on the minimum sphere, $r = r_o$, the sampling density in Eq. (4.1), as derived from the truncation criterion in Eq. (2.6), yields a distance of roughly half a wavelength between the (projected) sample points, in agreement with the sampling criterion for planar near-field measurements.

In addition to the angular sampling criteria, it must also be observed, that the minimum sphere for the AUT and the minimum sphere for the probe do not intersect each other (see Figure 1), since this situation would violate the transmission formula. This restriction can be expressed through the relation

$$\max(n)_{AUT} + \max(\nu)_{probe} < kA \tag{4.3}$$

4.2 Probe correction

Realistic probes do not detect the field at a single point, but rather some weighted average over the probe's aperture. If the probe cannot be assumed to behave very much like a *Hertzian* dipole, its influence must be properly accounted for. This is denoted *probe correction.*

If the probe has low directivity and the measurement distance to the AUT is 'not too close', then the probe may be assumed to be a *Hertzian* dipole, and probe correction can be ignored, since the received signal will be proportional to the electric field parallel to the polarization of the probe.

A necessary prerequisite for this probe correction is a knowledge of the probe's receiving characteristics as expressed through its coefficients $R^{p}_{\sigma\mu\nu}$, cf. Section 2.2.2. These must be determined from a separate measurement of the probe or, alternatively, from a numerical model of the probe.

The choice of a suitable probe depends on a number of parameters related to the set-up, the AUT and the transformation algorithm. Generally speaking the probe should not have a too low directivity, since then it will pick up undesired stray signals from sources not directly related to the AUT. Such a probe will also be sensitive to the structure on which it is mounted. A high directive probe may be used to suppress reflections and signals from sources outside the test zone (spatial filtering), while at the same time increasing the signal received from the AUT. The pattern from such a probe will be fairly independent of its nearby surroundings. The probe pattern should however not exhibit nulls or very low levels within the AUT minimum sphere.

If the Field-of-View (FOV) of the AUT as seen from the probe is large (short measurement distance/large AUT) , then a medium-to-low directive probe (approx. 8-12 dBi) is adequate, since the amount of multiple reflections between AUT and probe should be kept at a low level. A high directive probe might have low pattern levels within the test zone area, and could also cause a high level of multiple scattering. If the FOV is small (large measurement distance/small AUT) then a medium to high directive probe (approx. 13-17 dBi) is appropriate.

If the *Wacker/Jensen/Larsen* transformation algorithm is employed in the data processing scheme, then certain restrictions on the probe must be observed. As described in the Chapter prelude it is required that the probe's azimuthal pattern contains only the two harmonics with $\mu = \pm 1$, corresponding to a $\cos\phi$ and $\sin\phi$ azimuthal variation. This does not in any way limit the directivity of the probe, since this is related to the maximum value of the polar index ν. This type of probe can easily be manufactured e.g. as a circular waveguide or conical horn excited in the fundamental TE_{11} waveguide mode. The structure has the added advantage that it lends itself to dual-polarized operation, where the on-axis *polarization ratios* of the two ports are allowed to be different, but where the *patterns* radiated by the two ports are identical.

4.3 Alignment requirements

To achieve high accuracy in spherical near-field antenna testing one must pay careful attention to the alignment of the system.

As described in the Chapter prelude, the mechanical set-up shall provide for the three axes of rotation to comply with the geometrical requirements of spherical near-field antenna testing. Before initiating any measurement task, the system must be precisely aligned, therefore it must have built-in adjustment possibilities, and tools that facilitate the alignment, e.g. levellers, theodolites, mirrors, laser tracking interferometers, optical targets etc. . Mounting and dismounting of the AUT and probe must be precise and reproducible, and the mechanical parts must be sufficiently stable and rigid to ensure that the alignment is not altered when probe and/or AUT is rotated during the measurements.

Several different types of mechanical set-ups can be envisaged, many are already in use, and each one will typically require its own alignment procedures specially tailored to it.

In general therefore and only to be considered as a guideline, the axes should intersect each other within fractions of a wavelength, and at right angles typically on the order of hundredths of a decimal degree. Hence at very high frequencies (sub-millimetre range) it becomes much more involved to reach an acceptable accuracy.

5 Probes and probe calibration

This Chapter contains descriptions of different typical antennas used as probes for near-field antenna measurements. Advantages and disadvantages of different kinds of probes are pointed out. Parameters of the probes required by different probe-correction techniques for near-field antenna measurements are listed. Probe calibration procedures are described in detail for the presented kinds of probes.

5.1 Introduction

In near-field antenna measurements the field radiated by an Antenna Under Test (AUT) is first measured with an auxiliary antenna (probe) in a number of points on an imaginary surface located in the near field of the AUT. The measured field is then used to calculate the far-field characteristics of the AUT. The near-to-far field transformation algorithms require that two orthogonal complex (amplitude and phase) components of the field be measured at each point on the surface : two tangential orthogonal components of the electric field are usually required.

Any real antenna has a finite extent and when placed in the near-field of an AUT provides a signal, which is not directly proportional to the tangential component of the electric field. Thus, for accurate prediction of the far-field pattern of an AUT from a near-field measurement, correction for the probe characteristics is required [15]. The probe characteristics are typically determined from a separate measurement called probe calibration.

It is assumed in this document that both the AUT and the probe are reciprocal antennas. When this is not valid the characteristics of adjoint antennas are implied.

5.2 Requirements to the probes

The requirements to the probes are often contradictory and cannot be fulfilled completely. The requirements also vary depending on the measurement technique. There are, however, some general rules applicable to all probes for near-field antenna measurements (listed here not in the order of importance).

- The probe must keep/retain its characteristics with time and in different orientations with respect to gravity, such that its calibration results remain valid.
- The probe must have a well defined coordinate system, which can be accurately reproduced.
- The probe must be sensitive to the main field polarization and insensitive to the orthogonal field polarization.
- The probe must introduce minimum disturbance into the field being measured. (As one consequence of this requirement, the probe must be matched to its feed line – not strict, but desirable feature.)
- The probe itself shall present a low scattering cross-section (structural scattering) in the angular region towards the AUT in order to minimize the multiple scattering.

- The mounting structure supporting the probe including its feed line should be well covered with absorbers, or constructed in such a way that it ensures minimum scattering towards the AUT.

Several other features are not strictly required but rather useful:

- The probe should be wideband.
- The probe should be dual-polarized.
- The probe should have a standard interface to facilitate easy and fast interchanging with another probe.
- The probe should be lightweight.

It is also useful to apply a directive probe such that it suppresses undesired signals scattered from the environment. However, the directivity of the probe should be considered depending on the measurement technique.

In planar (rectangular or plane-polar) and cylindrical near-field measurement configurations it is desirable to have a probe with a large FOV, i.e. a pattern close to uniform over a solid angle close to a hemisphere towards the AUT (see Fig. 4a). It means that these probes should be low directive, unless only a limited angular region of the far-field is desired, in which case the probe can have a higher directivity.

In spherical near-field measurement configurations the probe is always pointing towards the centre of rotation of the AUT, and thus the uniform pattern is desired over a solid angle, which is essentially less than a hemisphere (see Fig. 4b). In this case it is useful to choose a more directive probe.

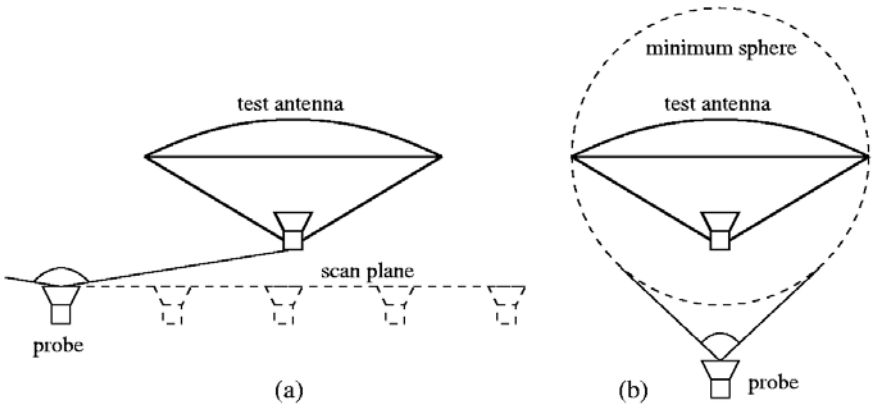

Figure 4: Illustration of the requirements to the probe pattern in (a) planar , and (b) spherical near field measurements.

5.3 Probe description and classification

It is convenient to divide the description of probes in two parts: first, typical radiating structures will be described and then attention will be paid to the feed networks.

5.3.1 Small dipoles and small loops

Small dipoles and small loops are sometimes used as probes in near-field antenna measurements. Their main advantages are that they introduce very small disturbances into the measured field and that their patterns are close to that of an ideal point source and thus pattern correction can often be omitted. Among the disadvantages, it should be mentioned that their input impedance is very low and it is thus difficult to match these antennas to a standard 50 Ω feed line. Wideband small dipoles and loops with resistive loading were described in a series of publications by Kanda, see e.g. [16]

5.3.2 Open-ended waveguide probes

One of the antennas often used as a probe in near-field antenna measurements is an open-ended waveguide. An open-ended rectangular waveguide (RWG) probe excited with the fundamental TE_{10} mode is particularly attractive because it is relatively wideband (approx. 1:1.5), very easy in production and inexpensive, and yet has very good characteristics. Its radiation pattern is wide in the E-plane and narrower in the H-plane. Rather simple approximate formulas for calculation of the radiation pattern of the RWG antenna have been derived [17]. Among the disadvantages of the RWG probe it should be mentioned that it cannot be made dual-polarized, unless it is made quadratic (in which case the bandwidth is reduced), and that the level of its backward radiation is quite strong. The last issue makes especially critical the design of absorbers covering the mounting structure: small changes in the absorber layout, due to dismounting and remounting, or properties, because of aging and transportation, may lead to noticeable changes in the radiation pattern. The open-ended RWG probes are available on the market from several vendors, e.g. MI-Technologies [18] and Orbit/FR [19].

An open-ended circular waveguide (CWG) probe is another widely used probe. It is typically characterized by a narrower bandwidth (approx. 1:1.3) as compared to the RWG probe. It should, however, be pointed out that the bandwidth can be increased by application of a specially designed feed network. There are two essential advantages of the CWG probe, which make it one of the best probes for planar and cylindrical near-field measurement configurations. First, it can be made dual-polarized, which allows to perform measurements of two orthogonal field components simultaneously. This, in turn, reduces overall measurement time and thus also reduces influence of the system drift on the measurement results. Second, the CWG probe excited by the fundamental mode of the circular waveguide (TE_{11}) represents a special class of probes called $\mu = \pm 1$ probes or first-order probes [5].

The properties of the first-order probes will be discussed later. It should also be mentioned that the feed network of the CWG probe, especially for a dual-polarized probe, is more complicated and thus more expensive as compared to the RWG probe feed network. A disadvantage of the CWG probe is the same as for the RWG probe: the level of backward radiation is quite strong. The open-ended CWG probes are available on the market from Orbit/FR [19].

An open-ended square waveguide probe has features and characteristics very close to the CWG probe, however, although being close to, it is not a first-order probe. The bandwidth is about the same. The detailed discussion will be omitted.

One of the disadvantages of the waveguide probes, the strong backward radiation, can be reduced by adding one or more chokes around the aperture. The aperture distribution becomes more symmetric, which results in more symmetric radiation patterns. The level of backward radiation is also decreased. Application of the choke(s), however, increases the cross-section of the probe and thus the possibility of increased back scattering towards the AUT. Also, a single choke is a narrow-band structure, whereas two-three chokes, being potentially wideband, are much more difficult to design and manufacture and further increase the back scattering towards an AUT. Application of modern advanced software tools with a capability to optimise a simulated object with respect to several parameters, such as radiation pattern and back scattering, allows designing an optimal probe. Several designs of such probes are available now on the market [18, 20, 21]. The cost of these is, indeed, much larger as compared to a simple open-ended waveguide.

Another disadvantage of a circular or square waveguide probe, their narrow bandwidth, can be improved by applying ridges. It is well known that a ridged waveguide has essentially increased bandwidth of the fundamental mode. Constructing a quad-ridged or quad-ridged circular or square waveguide probe thus allows making it both wideband and having minimum cross-section. Such probes are also available on the market [18]. On the other hand, it is not clear how such modifications influences the $\mu = \pm 1$ properties of the circular waveguide probes.

5.3.3 Conical and pyramidal horns

It was mentioned earlier that probes for spherical near-field measurement configurations may have a FOV essentially less than a hemisphere. In this case more directive antennas can be used as probes, such as small horn antennas. Formulas for design of a horn antenna can be found in any antenna handbook, but the manufacturing is more cumbersome as compared to a simple open-ended waveguide probe. A conical horn fed by a circular waveguide excited with the fundamental mode preserves the $\mu = \pm 1$ properties, and when implemented as a dual-polarized probe represents one of the best probes for spherical near-field measurement configurations [20]. A collection of such probes is employed at the DTU-ESA Spherical Near-Field Antenna Test Facility [22].

Pyramidal horns are, however, rarely used as probes for near-field antenna measurements. This is mainly due to the fact that these are essentially high-order probes, not well-suited for available near-to-far field transformation software, e.g. SNIFTD, which requires a first-order probe [20].

5.3.4 Other antennas

Several other kinds of antennas can be used as probes in near-field antenna measurements. To mention a few, a log-periodic antenna and a dielectric rod antenna are briefly described here.

A log-periodic antenna is sometimes used as probe for near- and far-field antenna measurements. However, it is considered as being not very suitable for the purpose because of its high level of cross-polarization or, in other words, because of high sensitivity to the undesired orthogonal field

component. On the other hand, a log-periodic antenna can be constructed to be dual-polarized and also extremely wideband, e.g. up to 1:25 or even more. These two features make this antenna deserve special attention.

A dielectric rod antenna is another example of a dual-polarized wideband probe. Information on this interesting antenna is quite limited, but it is believed that further investigations should make this antenna another good candidate as probe for near-field antenna measurements.

5.3.5 Feed networks

For small dipoles and small loops the feed network represent a major problem, since first, it should match low input impedance of the dipole or loop with a standard feed line, and second, it should provide a transition from a symmetric antenna to a typically non-symmetric feed line. Several designs can be found in the literature, but are not discussed here.

The feed network of RWG probe is usually made as a simple coax-to-waveguide transition.

The feed network of CWG probe can be made in several ways.

- As usual coax-to-rectangular waveguide transition in conjunction with a co-axial or perpendicular rectangular-to-circular waveguide transition.
- As two oppositely located monopoles with a 0°/180° hybrid power splitter, or with an in-phase power splitter but with cables of different lengths to ensure excitation of the monopoles with opposite phases at a specified frequency, typically at the centre of its operating band
- Special design including ridges [18, 21], and other.

5.4 Calibration parameters

As is evident from the description of the probes above, there exist many different kinds of probes with their own advantages and disadvantages. Considering the probes from the viewpoint of their calibration, they will be classified here in the following way:

- Small, single/dual polarized probes – probes with the overall size essentially smaller than the wavelength, such that the pattern can be assumed to coincide with the pattern of an ideal point source/receiver (Electric or Magnetic Hertzian dipole).

- Large, first-order ($\mu = \pm 1$) single/dual polarized probes – probes with the overall (aperture) size comparable to or larger than the wavelength, and with the azimuthal pattern dependence having only the first-order ($\cos\phi / \sin\phi$) dependence. Open-ended circular waveguides excited with the fundamental TE_{11} mode and conical horns fed by such a waveguide belong to this kind of probes (see detailed description in [5]).

- Large, high-order single/dual polarized probes – probes with the overall (aperture) size comparable to or larger than the wavelength and with the azimuthal pattern dependence having arbitrary (high-order) dependence.

The following characteristics are required for all frequencies of interest and for all kinds of probes:

- gain (if required),
- for dual-polarized probes : channel balance, i.e. the amplitude/phase difference between the ports,
- reflection coefficient.

The need for the pattern and the polarization characteristics (axial ratio, tilt angle, sense of rotation) depends on the probe category according to the classification above :

- for small single/dual-polarized probes the pattern is assumed to coincide with that of a point source; polarization characteristics for each port are required,
- for large first-order ($\mu = \pm 1$) single/dual-polarized probes the E- and H-plane patterns are required for one port (the two ports are assumed to radiate the same pattern); polarization characteristics for each port are required,
- for large high-order single/dual polarized probes complete patterns for each port are required; polarization characteristics for each port are not required since this information is contained in the pattern.

5.5 Calibration procedures

5.5.1 Gain calibration

The gain calibration for all kinds of probes can be carried out by any of the available techniques, such as 3-antenna far-field gain calibration [1], gain-transfer (substitution) far-field technique [1], gain-transfer (substitution) near-field technique [5, pp. 210-214], or 3-antenna near-field gain extrapolation technique [23].

5.5.2 Polarization calibration

The polarization characteristics for small and large first-order probes can be determined by the three-antenna method described in [1, 5 pp. 160-161]. Alternatively, these can be determined from a polarization measurement made with a polarization-calibrated antenna [5, pp. 157-160]. The far field conditions shall apply during the calibration. The polarization characteristics shall be determined for each port of the probe.

For large high-order probes the complete pattern calibration is carried out with a polarization calibrated auxiliary antenna (see Section 5.5.4 *Pattern calibration* below). The polarization characteristics of the probe are thus included in the complete probe pattern data, and a separate polarization calibration of the probe is not required.

5.5.3 Channel balance (for dual-polarized probes)

The channel balance of a dual-polarized probe is determined from a single polarization scan made with a linearly polarized antenna [5, pp. 161-163]. The far field conditions shall apply during the measurement. The data from the polarization characteristics measurement can be re-used for this purpose. Preferably the channel balance measurement should be carried out after the probe is connected to the measurement system, since the different reflection coefficients of the load and/or different characteristics of the two channels of the measurement system may impact the channel balance. Alternatively, it must be ensured that the reflection coefficient of the probe load is the same both during the calibration and during the use of the probe, and that the difference between the channels is taken into account.

5.5.4 Pattern calibration

For small probes the pattern calibration is not required, since the pattern can be assumed to coincide with the pattern of an ideal point source/receiver (Electric or Magnetic Hertzian dipole).

For the first-order probes, only E- and H-plane cuts of the pattern are required. The complete pattern can then be reconstructed from these two cuts, see [5, p.150]. The E-plane and H-plane pattern cuts can be measured under far field conditions by a polarization matched linearly polarized antenna. Alternatively, an iterative procedure described in [5, p.71-73] can be applied. The spacing between the polar pattern samples should be chosen not larger then:

$$\Delta\theta = 360^\circ / (2N+1) \tag{5.1}$$

where $N = kr_o + 10$, with r_o being the radius of the minimum sphere completely enclosing the probe, cf. the discussion in Section 2.2.1. For the high-order probes, the complete pattern calibration is required. The spacing between the polar pattern samples should be chosen according to the guidelines above. The spacing between the azimuthal pattern samples can be chosen equal to the same value, or smaller, if the smallest cylinder parallel to the *z*-axis and enclosing the probe has radius $R_o \left(\leq r_o\right)$ **:**

$$\Delta\phi = 360^\circ / (2M+1) \tag{5.2}$$

where then $M = kR_o + 10$.

The pattern calibration of the auxiliary antenna can be omitted if the probe calibration is done under far field conditions. If the probe calibration is done under near-field conditions, full pattern and polarization correction of the auxiliary antenna is required.

5.5.5 Reflection coefficient

The reflection coefficient of each probe port shall be measured with a calibrated network analyzer in an anechoic environment.

6 Probe arrays

Probe arrays are commonly used in near-field antenna measurement systems predominantly due to the increased measurement speed with respect to conventional single probe measurement systems [24, 25, 26]. In all near-field measurement applications (spherical, planar, cylindrical, etc) the time required to physically move the measurement probe for each sampling step is the main contributor to the overall measurement time. Using a probe array one or more mechanical axes are substituted with fast electronic scanning of the array, leading to a significant reduction in the overall measurement time. The theoretical time reduction obtained with a probe array is equal to the number of probes employed in the probe array. Probe arrays employing more than a hundred elements are quite common providing orders of magnitude improvements in measurement speed for typical antenna measurement applications.

6.1 Spherical geometry

In the spherical geometry, the conventional single probe system and the probe array system both perform a 3D measurement of the near-field surrounding the antenna and both approaches employ conventional near-field to far-field transformation techniques to determine the far-field pattern radiated by the antenna under test [5]. For the single probe system, a full 3D sampling of the antenna near-field requires two mechanical axes of movement as shown in Figure 5a. Using a probe array, as illustrated in Figure 5b, one mechanical axis is substituted with fast electronic scanning of the array leading to a significant reduction in the overall measurement time.

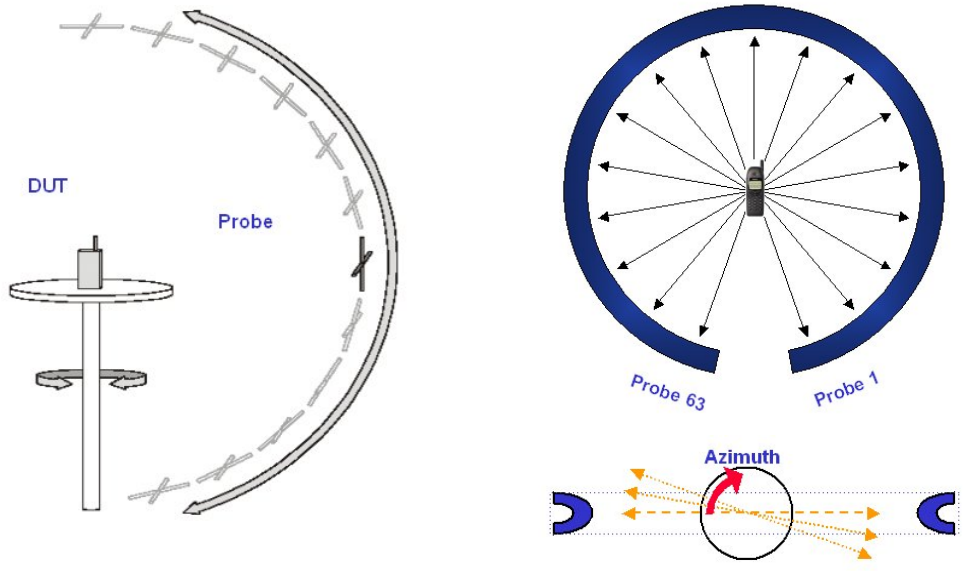

a) Conventional single probe system b) Probe array system

Figure 5: Comparison of the conventional single probe measurement system with two mechanical axes (azimuth and elevation) and the probe array based system with electronic scan in the elevation dimension and mechanical scan in the azimuth dimension.

6.2 Probe array implementation

In order to retrieve the measured amplitude, phase and polarisation information from each probe of the probe array a high frequency multiplexing network could be used. However this solution is rather expensive for even a limited number of probes and requires a separate cable from probe to multiplexing unit. A better way to proceed is the patented measurement concept: Advanced Modulated Scattering Technique (A-MST) [27] employed by SATIMO [24, 25, 26] in their spherical near-field measurement systems.

The A-MST allows identifying the signal from each probe in the probe array by perturbing the electromagnetic properties of the interrogated probe. This perturbation can be introduced by a low frequency modulator operating in the kHz frequency range, enabling the use of standard low cost electronic components. The result of this perturbation is a modulation frequency component in the output signal which is directly related to the amplitude and phase of the incident field at the location of the probe. By sequentially modulating each probe in the probe array it is possible to measure, in virtually real time, the amplitude and phase at each probe location without the need for an expensive high frequency multiplexing network. The low frequency modulator is synchronized with the receiver data acquisition to provide phase and amplitude measurements at each probe in fractions of a millisecond. The arrays of sensors can then be connected to the receiving equipment through a simple passive power dividing network. The concept is illustrated in Figure 6.

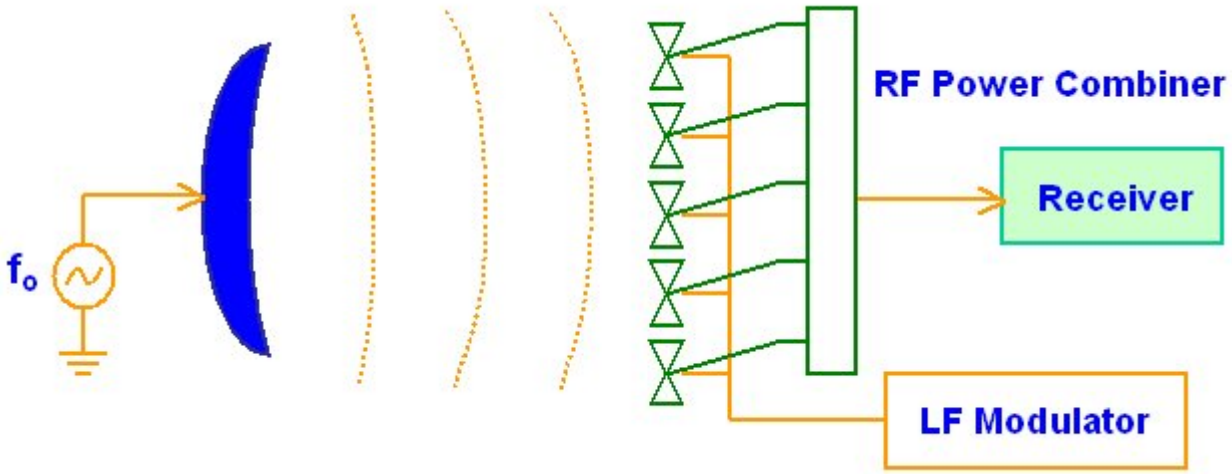

Figure 6: Illustration of the A-MST. The probes are connected to the receiver through the same cable. A low frequency modulation allows identifying the signal from each probe in the probe array by perturbing the electromagnetic properties of the interrogated probe.

6.3 Error sources particular to probe arrays

Potential users of probe array systems are often concerned with the level of uncertainties related to effects from coupling among the probes. A high coupling level would be destructive to the probe array performance, since these effects vary with different antenna under test (AUT) and between calibration configuration and test configurations.

In general, probe to probe coupling can occur via various paths. In the following we will define a set of terms used to describe the general coupling phenomenon and how these contributions have been minimized in the implementation of the A-MST probe arrays in the commercial SATIMO SG system [24, 25, 26]. Furthermore, special error terms and their minimization through calibration, deriving from the mechanical implementation of the probe array systems are also treated.

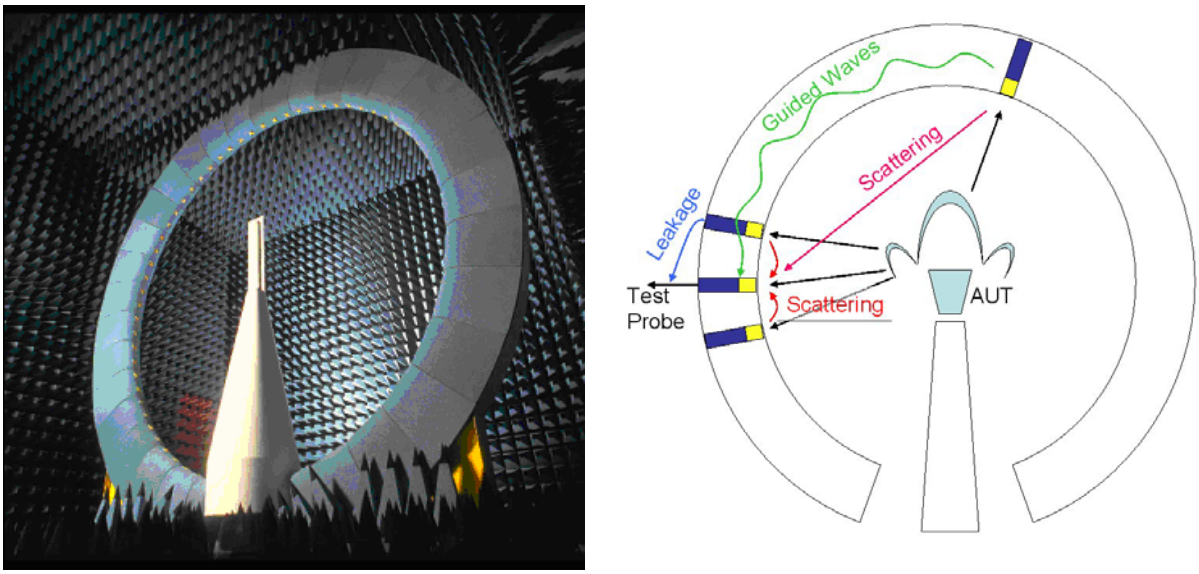

Figure 7: Example of probe array implementation (left) and error sources particular to probe arrays (right).

6.3.1 Internal Leakages

Coupling between probes can occur via leakage through the combiner network and is a function of the efficiency of the modulation scheme in an A-MST system or the isolation of the switches in a switched array system. Measurements on the commercial SATIMO SG system [24, 25, 26] based on A-MST show this coupling level to be less than -100dB from the direct path.

6.3.2 Local External Mutual Scattering

As in all measurement systems the measurement probe will receive a part of the incident signal and scatter the rest. Some of the scattered field will be received by neighbouring probes in a probe array implementation. In array antennas this is sometimes referred to as mutual scattering and also often

referred to as mutual coupling. This coupling is seen as a distortion of the isolated probe pattern when embedded in the array. It is well known that the probe pattern shape is a relatively small uncertainty contributor when wide angular probes are used with moderate sized AUTs. Measurements of embedded radiation patterns of probe arrays in the commercial SATIMO SG system [24, 25, 26] show that this condition is always respected.

6.3.3 Distant External Coupling

This coupling phenomenon is observed as an increase in the general reflectivity level in the quiet zone and can be measured using normal quiet zone scanning techniques. With multilayer conformal absorbers and low scattering cross section probes, the implementation of A-MST probe arrays in the commercial SATIMO SG system [24, 25, 26] reduces this effect to levels comparable to the general anechoic chamber reflectivity levels.

6.3.4 Guided Wave Coupling

Probe arrays, being periodic and complex structures, can support guided waves that lead to probe coupling. Such guided waves can occur as trapped energy inside hollow sections of the array or surface waves similar to what is observed in array antennas. In early probe arrays this coupling phenomenon has turned out to be a significant source of uncertainty. However, prudent probe array design can eliminate these coupling waves.

6.3.5 Probe Array Mechanical Distortion

Ideally speaking all probes of a probe array should be located on an ideal circle. Obviously, manufacturing tolerances for probes and the probe array fixture in a probe array implementation are finite, so some distortion will occur to the effective radial position and pointing direction of each probe. This distortion is predominately static and can be compensated in the probe array calibration process (see below). The positioning and pointing errors of each probe cannot be compensated and should be minimized in the mechanical design of the probe array. While the on-axis radial position errors are completely compensated by the probe array calibration, the effects of the off-axis radial errors are significantly improved as illustrated by the following formula:

$$\Delta R_{cal} = \Delta R_{physical} \cdot (1 - \cos(\varphi)) \tag{6.1}$$

in which ΔR_{cal} is the resulting worst case effective radial positioning error due to a physical radial error $\Delta R_{physical}$ and φ is the half angle containing the AUT as seen from probe. Thus, if the AUT fills a field-of-view seen from the probe of ±30°, then we have approximately a tenfold improvement in the radial positioning error from the probe array calibration.

6.4 Probe Array Calibration

The individual probes of a probe array system are often mass produced to limit the overall cost of the system. Although good mechanical accuracies can be achieved in quality mass production, some imperfections in the polarisation alignment and the low frequency modulation components of an A-MST system or in the switching network of a switched array system are to be expected. The probe array calibration serves to compensate such imperfections in the manufacturing and mounting of each individual dual-polarized probe. Although the un-calibrated probe's performance is often intrinsically reasonable a significant improvement in probe response can be obtained from the proper calibration scheme with very little effort.

The commercial SATIMO SG system [24, 25, 26] employ wide-band probes with bandwidths ranging from 1:15 to 1:36, and the probes are mass produced to limit the overall cost of the system. After installation, each probe is calibrated by pointing a linearly polarized horn antenna towards each of the probes in the probe array as shown in Figure 8a. Dual-polarized, phase and amplitude measurements are taken as the horn is rotated in front of each probe rotating the incident polarisation axis as shown in Figure 8b. By applying a Fourier transform of the recorded data in azimuth the polarisation orientation of each individual probe can be accurately determined. The recorded data also serves to align the amplitude and phase response of each probe with frequency.

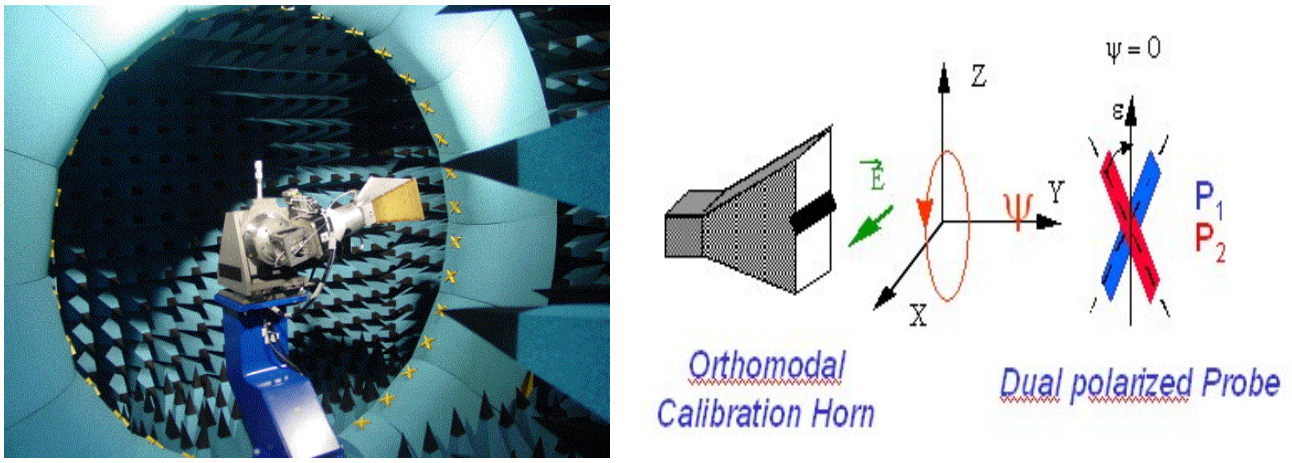

Figure 8: Probe calibration implementation (left). Schematics of the probe calibration procedure for each individual probe in the probe array (right).

From the calibration process outlined above, a set of calibration coefficients are derived for each probe. The calibrated H and V components of the electromagnetic field are obtained from the measurements due to the imperfect probe (M_1, M_2) by the following equation:

$$\begin{pmatrix} V \\ H \end{pmatrix} = \begin{pmatrix} Y_{11} & Y_{12} \\ Y_{21} & Y_{22} \end{pmatrix} \begin{pmatrix} M_1 \\ M_2 \end{pmatrix} \tag{6.2}$$

The [Y] coefficient matrix is able to compensate for differences among probes, align the polarization axes, and reduce the cross-polarization components. After calibration, the typically measured probe uniformity measured as the amplitude and phase response of each probe to the same stimulus is better than ±0.1dB and ±0.5° throughout the entire bandwidth. The probe co-polar to cross-polarisation response ratio is close to 40dB after calibration as shown in Figure 9, which illustrates the co-polar /cross-polar response for the entire array before and after probe calibration with probe number along the X-axis.

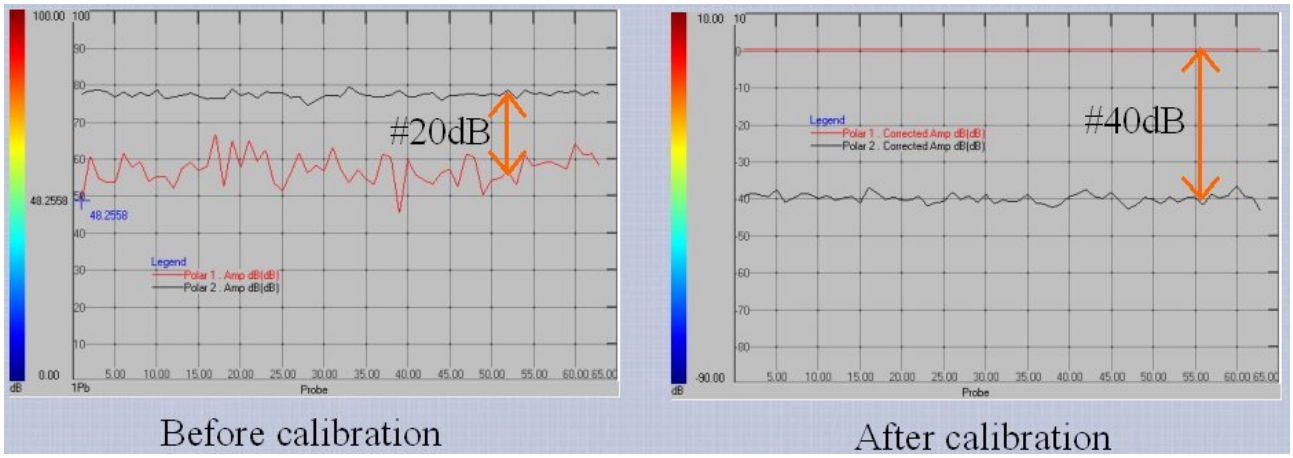

Figure 9: Co-polar /Cross polar performance with probe number along the X-axis for a typical probe array before (left with about 20dB ratio) and after probe calibration (right with close to 40dB ratio).

7 References

[1] IEEE Standard Test Procedures for Antennas, IEEE Std 149-1979.

[2] IEEE Standard Definitions of Terms for Antennas, IEEE Std 145-1993.

[3] M. Francis et al., "IEEE Recommended Practices for Near-Field Antenna Measurements", Draft IEEE Standard, 2005.

[4] R.C. Baird, A.C. Newell, and C.F. Stubenrauch, "A Brief History of Near-Field Measurements of Antennas at the National Bureau of Standards", IEEE Trans. Antennas Propagat., Vol. AP-36, pp. 727-733, June 1988.

[5] J.E. Hansen, (Ed), "Spherical Near-Field Antenna Measurements", Peter Peregrinus, Ltd., on behalf of IEE, London, 1988.

[6] E.B. Joy, "A Brief History of the Development of the Near-Field Measurement Technique at the Georgia Institute of Technology", IEEE Trans. Antennas Propagat., Vol. AP-36, pp. 740-745, June 1988.

[7] J. Brown and E.V. Jull, "The Prediction of Aerial Radiation Patterns from Near-Field Measurements", Proc. Inst. Elec. Eng., Vol. 108, part B, no. 42, pp. 635-644, Nov. 1961.

[8] A. Frandsen and F. Jensen, "On The Number Of Modes In Spherical Wave Expansions", Proc. of the 26th AMTA Symposium, Atlanta, pp.489-494, 2004.

[9] D. M. Kerns, "Plane-wave scattering matrix theory of antennas and antenna-antenna interactions : formulation and applications", J. Res. NBS, **Vol. 80B**, No. 1, pp. 5-51, 1976.

[10] P.F. Wacker, "Non-planar near-field measurements : Spherical scanning", Report **NBSIR 75-809**, Electromagnetics Division, Inst. for Basic Standards, NBS, Boulder, Colorado, 1975.

[11] F. H. Larsen, "Probe-corrected spherical near-field antenna measurements", Ph.D. Thesis, Electromagnetics Institute, Technical University of Denmark, Report **LD36**, 1980.

[12] P.F. Wacker, "Near-field antenna measurements using a spherical scan: Efficient data reduction with probe correction", Conf. on Precision Electromagnetic Measurements, IEE Conf. Publ. No. 113, pp. 286-288, London, UK, 1974.

[13] T. Laitinen, S. Pivnenko, O. Breinbjerg, "Aspects of probe correction for odd-order probes in spherical near-field antenna measurements", Proc. of the 26th AMTA Symposium, Atlanta, pp.98-103, 2004.

[14] F. Jensen, "On the probe compensation for near-field measurements on a sphere", Archiv für Elektronik und Übertragungstechnik, Vol. 29, No. 7/8, pp. 305-308, 1975.

[15] A. D. Yaghjian, "An overview of near-field antenna measurements", IEEE Trans. Antennas Propagat., Vol. AP-34, pp. 30-45, Jan. 1986.

[16] M Kanda, "Standard probes for electromagnetic field measurements", IEEE Trans. Antennas Propagat., Vol. AP-41, pp. 1349-1364, Oct. 1993.

[17] A. D. Yaghjian, "Approximate formulas for the far-field and gain of open-ended rectangular waveguide", IEEE Trans. Antennas Propagat., Vol. AP-32, pp. 378-384, Apr. 1984.

[18] MI-Technologies, www.mi-technologies.com/Microwave_Components/Probes.htm

[19] Orbit/FR, www.orbitfr.com

[20] TICRA, www.ticra.com

[21] SATIMO, www.satimo.com

[22] DTU-ESA Antenna Test Facility, www.emi.dtu.dk/research/afg/snf/SNF.html

[23] A. Newell, R. Baird, P. Wacker, "Accurate measurement of antenna gain and polarization at reduced distances by an extrapolation technique", IEEE Trans. Antennas Propagat., Vol. AP-21, pp. 418-431, July 1973.

[24] P.O. Iversen, Ph. Garreau, K. Englund, E. Pasalic, O. Edvardsson, G. Engblom, "Real Time Spherical Near Field Antenna Test Range for Wireless Applications", Proceedings of AMTA 1999 – Antenna Measurement Techniques Association, pp. 363 – 368, October 4-8 1999, Monterey Bay, California.

[25] L. Duchesne, Ph. Garreau, N. Robic, A. Gandois, P.O. Iversen, G. Barone, "Compact multi-probe antenna test station for rapid testing of antennas and wireless terminals", 4th Mediterranean Microwave Symposium, Marseille 2004.

[26] Ph. Garreau, L. Duchesne, A. Gandois, L. Foged, P. Iversen "Probe array concepts for fast testing of large radiating structures", AMTA 2004, Atlanta Georgia.

[27] J.-C. Bolomey, F.E. Gardiol, "Engineering Applications of the Modulated Scatterer Technique", Artech House, Boston, 2001.